Hindawi
Advances in Materials Science and Engineering
Volume 2022, Article ID 9594798, 7 pages
https://doi.org/10.1155/2022/9594798

Research Article

Investigations on Wear Behavior of Aluminium Composites at Elevated Temperature

B. R. Senthil Kumar,[1] G. Gopalarama Subramaniyan,[2] N. Pragadish,[3] P. M. Venkatesh,[4] Soni Sanjay,[5] C. M. Velu,[6] G. Navaneethakrishnan,[7] Suresh Vellingiri,[8] and Venkatesan Govindarajan[9]

[1]*Nehru Institute of Engineering and Technology, Coimbatore, Tamil Nadu, India*
[2]*Saveetha Engineering College, Chennai, Tamil Nadu, India*
[3]*Vel Tech Multitech, Avadi, Chennai, Tamil Nadu, India*
[4]*Vignan's Foundation for Science Technology and Research, Guntur, India*
[5]*Jabalpur Engineering College, R.G.P.V.Bhopal, Jabalpur, Madhya Pradesh, India*
[6]*Saveetha School of Engg, Saveetha Institute Medical and Technical Sciences, Saveetha University, Chennai, Tamil Nadu, India*
[7]*QIS College of Engineering and Technology, Ongole 523272, Andhra Pradesh, India*
[8]*Department of Mechanical Engineering, Adhi College of Engineering and Technology, Kanchipuram, Tamil Nadu, India*
[9]*Department of Mechanical Engineering, Haramaya Institute of Technology, Haramaya University, Dire Dawa, Ethiopia*

Correspondence should be addressed to Venkatesan Govindarajan; venkatesanggg2011@gmail.com

Received 13 April 2022; Revised 19 May 2022; Accepted 10 June 2022; Published 27 June 2022

Academic Editor: Vijayananth Kavimani

The aerospace aluminium alloy AA7050 was reinforced with Al_2O_3 of average particle size 5 m in this study using the stir casting method. To eliminate surface imperfections, AA7050/Al_2O_3 composites with varied weight percentages (0, 2, 4, 6) were manufactured, and wear tests on composites were carried out utilizing a pin-on-disc apparatus that varied load, velocity, temperature, and weight %. The tensile and hardness tests were carried out at a high temperature. The inclusion of particles enhances wear resistance by establishing a mechanically mixed layer (MML), according to the findings. The wear resistance at 300°C was 100% higher in comparison with resistance at 150°C. Because of the Orowan strengthening and Hall–Petch effect, the tensile strength and hardness of composites enhanced. Temperature, tracked by the weight % of strengthening powders, was the most important factor that influences the wear resistance of the composites. The findings showed that the material properties of AA7050/4wt%Al_2O_3 at 150°C and AA7050/2wt%Al_2O_3 at 300°C are superior than base alloy.

1. Introduction

AA7050 alloy has piqued attention across the globe in latest generations as the extremely ideal material for aerospace application, owing to its enhanced mechanical, tribological, and corrosion behavior [1]. Due to the growing need for lightweight materials in both developed and developing nations, defect-free composite materials are in high demand [2]. The quality of the materials used in any aerospace system determines its effectiveness. Some of the aerospace components manufactured by aluminium alloy are the hot plate collector, isolator, mount, thermal ducts, header pipeline, and moulding [2–5]. Since the sunlight-based header pipelines were accessible to high temperatures, it was necessary to investigate their viability at elevated temperatures [6].

Particles such as B_4C, SiC, WC, Al_2O_3, and Gr are used to strengthen aluminium alloys [7–9]. Sintering, moulding, and in situ production are the most often utilized composite manufacturing procedures [10–12]. The stir casting method was the most suitable of the numerous manufacturing procedures for mass production and uniform particle

Table 1: Elemental proportion of AA7050 aluminium alloy.

Zn	Mg	Cu	Fe	Cr	Si	Mn	Al
6.30	2.58	1.83	0.28	0.27	0.06	0.05	Balance

dispersion [13, 14]. The molten metal was stirred at a constant speed for a specified period of time utilizing a mechanical mixer [15]. The wettability of composites was improved by adding preheated particles [16].

The wear of the materials is governed by the velocity, sliding distance, load, temperature, and counterface hardness [17–19]. The impact of addition of SiC particles on the wear rate of aluminium composites was investigated. The addition of SiC particles increases the tribological capabilities, according to the findings. B_4C particles upsurge the strength, stiffness, and wear endurance of the AA2020 alloy [20]. When the load was increased over 60 N, the mild to severe regime transitioned. Sardar et al. found that hybrid composites had superior wear resistance than single-reinforced composites [21]. Increased matrix fortification improves elasticity, yield strength, and hardness [22]. The microhardness of the composite rises as the Al-N proportion in the alloy matrix increases [23]. The amalgamation of SiC and Al_2O_3 increases the composites' hardness, tensile strength, and density [24].

From the above survey, it was revealed that a significant amount of research has been done on the tribological performance of composites. However, only a few analyses have been performed on the tribological behavior of AA7050 composite materials at high temperatures. The objective of this study was to reinforce AA7050 alloy with Al_2O_3 particles and test wear behavior on reinforced composite materials at elevated temperatures. The mechanical and tribological properties of the composites were studied at high temperatures. With the use of an ANOVA table, the most influential factor was identified.

2. Experimental Procedure

Table 1 displays the elemental position of the AA7050 aluminium alloy as established by spectrochemical analysis. The liquid stir casting process was used to strengthen the AA7050 alloy with aluminium oxide (Al_2O_3) grains with a mean size of 5 μm. Around 1 kg of alloy was placed in a graphite receptacle and charged to 870°C in an electric furnace made by TSR instruments and solutions, according to the process parameters listed in Table 2.

Before being introduced to the charge, Al_2O_3 was charged to a temperature of 250°C to eradicate any moisture. The liquid was stirred for 4 minutes at 600 rpm using a sieve shaker. To increase wettability, an equivalent weight percentage of potassium titanium fluoride (K_2TiF_6) was introduced to the melt. The combination was agitated for additional 3 minutes after the flux was added. Figure 1 depicts the step-by-step technique entangled in the manufacture of composites.

Composites with dimensions of (−12 mm × L−105 mm) were made from the combined slurry which was put into a warmed die steel mould. To eliminate the surface defects, the specimens were turned and faced to a dimension of diameter 10mm × length 100mm. Wear tests on composites were completed as per ASTM-G99 principles by differing the temperature, stress, speed, and weight % of the composites utilizing a pin on plate contraption created by Ducom instruments; exploratory runs were arranged utilizing a Taguchi blended symmetrical exhibit.

Table 2: Casting variables.

Parameters	Value
Pouring temperature	870°C
Preheating temperature of Al_2O_3	250°C
Preheating temperature of mould	250°C
Stirring time	7 min
Stirring speed	600 rpm

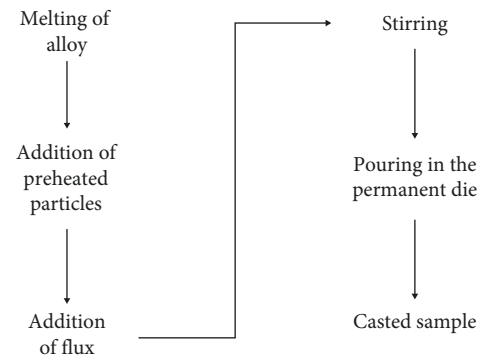

Figure 1: Steps involved in the production of composites.

The worn track was 100 mm in diameter, and the counterface was made up of EN-31 steel. The Taguchi orthogonal array was used to create the wear trial runs, which were then repeated three times. A Rockwell hardness tester and a universal testing machine were utilized to assess the composites' hardness and tensile strength at increased temperatures, according to ASTM-E18 and ASTM-E21 standards, respectively. The Rockwell hardness tester and UTM were manufactured by Xtreme Engineering Equipment Private Limited and Hualong, respectively. The hardness of nonferrous alloys was evaluated with a load of 100 N and a dwell time of 15 seconds, as specified by ASTM, and the outcomes were documented in Rockwell B-Scale. The specimen was placed in the UTM with a notch radius of 12.5 mm and a length and width of 50 mm and 4 mm, respectively. The load was added progressively until the material broke down at the specified temperature. Each experiment was conducted on three separate samples, with the average value being documented as the investigational findings. The most influential factor was revealed using an ANOVA (Table 3).

Table 3: Wear process parameters and their levels.

Process parameters	Levels
Reinforcement percentage	0, 2, 4, 6
Applied load (N)	15, 30
Speed (m/s)	15, 30
Temperature (°C)	150, 300

3. Results and Discussion

Figure 2 illustrates the microstructure of the composites. The Al2O3 particles were equally spread over the matrix material, according to the structure. The presence of a white film surrounding the reinforced particles suggests that Ti was applied to the reinforced particles. K2TiF6 flux was used to remove this titanium. The wear proportion of composites diminishes with the incorporation of reinforcing particles till four weight percent, after which it increases, according to the experimental data. The average wear proportion of amalgams was 7% inferior than that of unreinforced alloy, 629 mg for pure metal and 588 mg for composites reinforced with 4% Al_2O_3 particles, according to the Archard equation (equation (1)). The particles on the surface of the composites get dislodged during sliding and reach the contact region. Both metals are abraded by the ceramic particles, resulting in the formation of a MML [25]. The presence of Fe in the worn surface was confirmed through EDAX analysis, which reveals that the materials were mechanically mixed and averts direct metal surface contact as depicted in Figure 3. This MML hangs between the contact surfaces, averting metal surface contact and thereby reducing wear. When the temperature is rapidly increased from 150°C to 300°C, the wear rate increases by 100% as shown in Figure 4.

When sliding at 300°C, the material achieves its deformation state and becomes significantly deformed, resulting in increased material loss. At high temperatures, the parameters load and velocity have little effect on wear rate. The friction coefficient (COF) decreases to 0.166 as a result of the deformation condition, which is 40% less than materials sliding at 150°C as shown in Figure 5. All other variables have a minor or no effect on COF.

$$W = K\left(\frac{PLV}{3H}\right), \tag{1}$$

where P represents the applied load in N, L represents the sliding distance in m, V represents the applied velocity in m/s, H represents the hardness in HRB, and K represents the experimental constant.

The tensile strength of the AA7050/Al_2O_3 composites at high temperatures is shown in Figure 6. The composites with 4% reinforcement exhibited the highest tensile strength at 150°C. Orowan strengthening [26] induced the rise in strength, which indicates that the particles in the matrix give resistance to the movement of dislocation. The alloy reinforced with 2 weight % provides good tensile strength at 300°C.

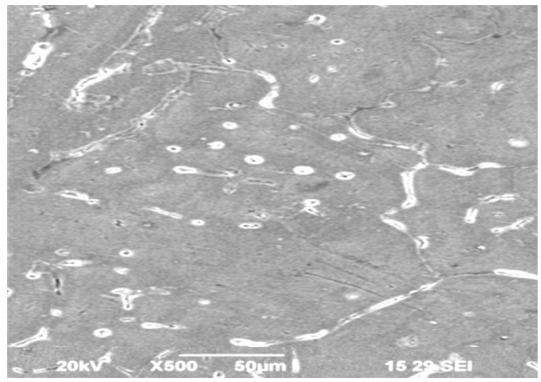

Figure 2: Microstructure of AA7050/Al2O3 composites.

$$\begin{aligned}\text{Wear} = {} & 163.000 + 15.5625\ \text{Weight percentage} \\ & - 1.13333\ \text{Load (N)} + 1.25000\ \text{Velocity (m/s)} \\ & - 0.348333\ \text{Temperature (C)} \\ & - 0.843750\ \text{Weight percentage} * \text{Weight percentage} \\ & - 0.483333\ \text{Weight percentage} * \text{Velocity (m/s)} \\ & + 0.0111111\ \text{Load (N)} * \text{Velocity (m/s)}.\end{aligned} \tag{2}$$

When the temperature is increased from 150°C to 300°C, the tensile strength is reduced by 95%. When a material is heated to a high temperature, its viscosity drops, resulting in an increase in percent elongation and a loss in tensile strength [27, 28]. The findings revealed that adding reinforcement had the least impact on tensile strength at high temperatures, and that material property loss was linked to viscosity drop at high temperatures [29, 30].

Figure 7 shows how adding Al_2O_3 particles increases the composites' toughness [31, 32]. The flux's titanium element encircles the reinforcing particles, prompting them to bind together. The titanium element refines the grain size due to the Hall–Petch effect, which raises the hardness value. The hardness of AA7050/6Al_2O_3 was 16% higher at 150°C than that of the unreinforced alloy and 11% higher at 300°C. When the temperature was raised to 300°C, the hardness value dropped by 75% [33, 34]. As indicated in Table 4, the most influential factor influencing material property is temperature, followed by weight reinforcement.

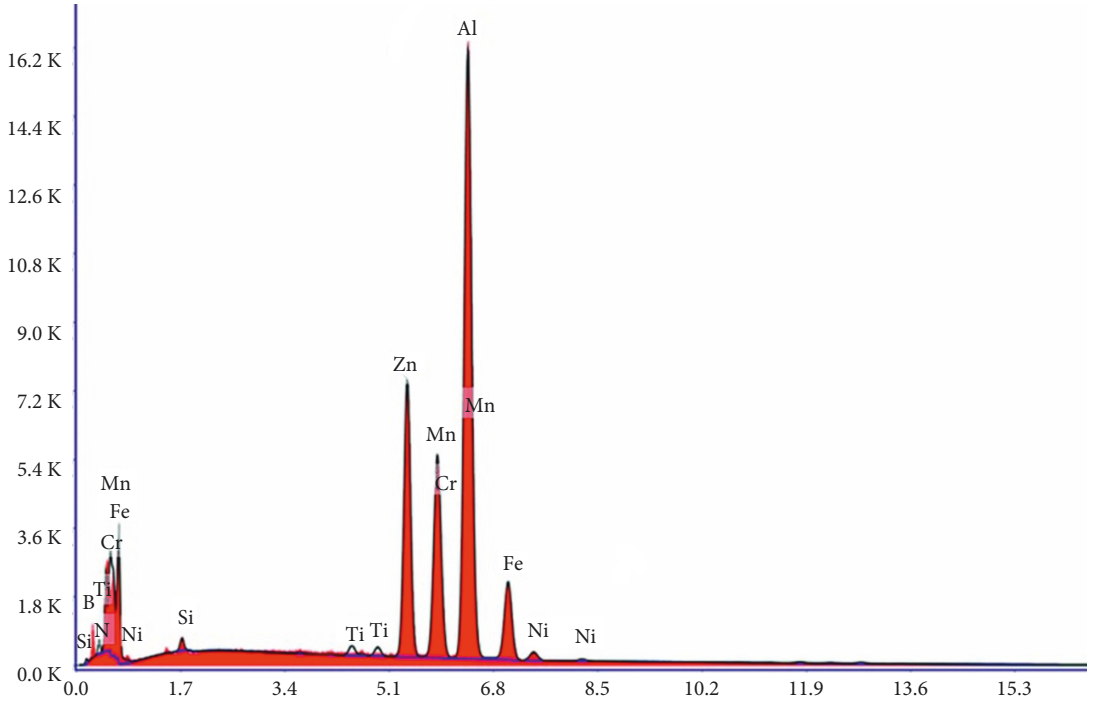

Figure 3: EDAX of worn surface of AA7050 composites.

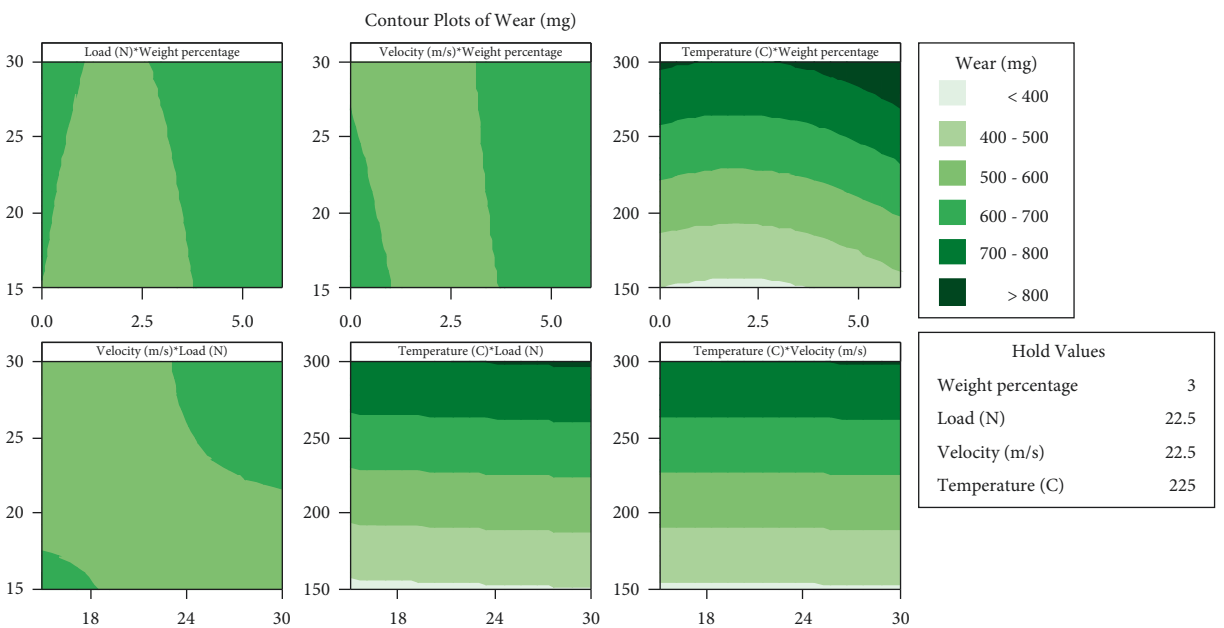

Figure 4: Interaction impact of various process parameters on wear of AA7050/Al2O3 composites.

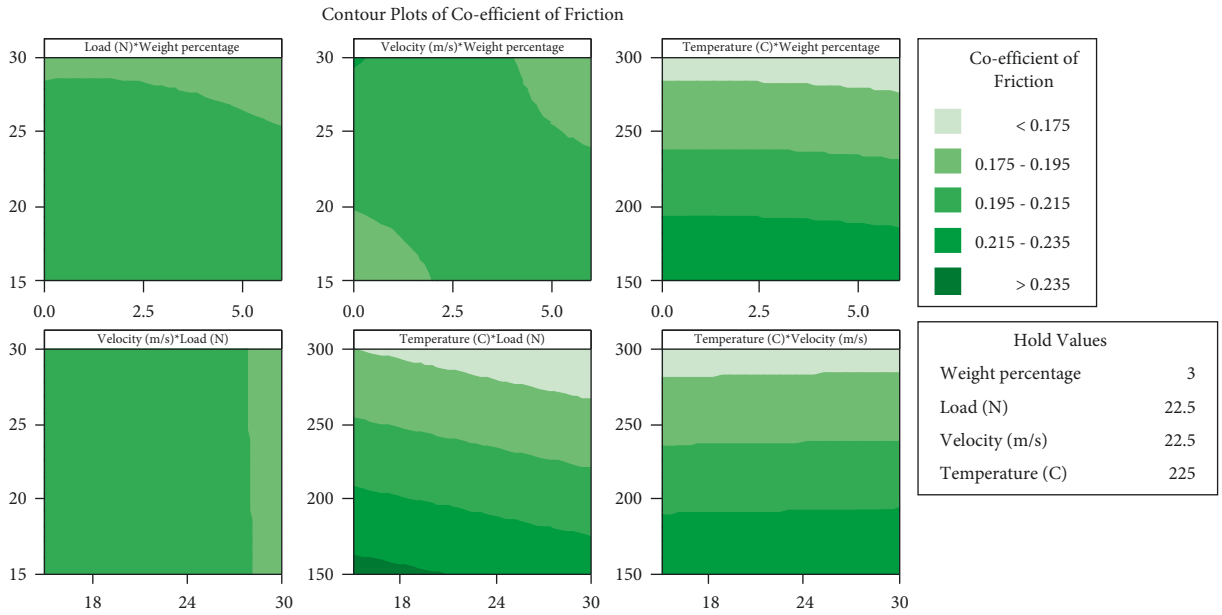

Figure 5: Interaction impact of various process parameters on COF of AA7050/Al2O3 composites.

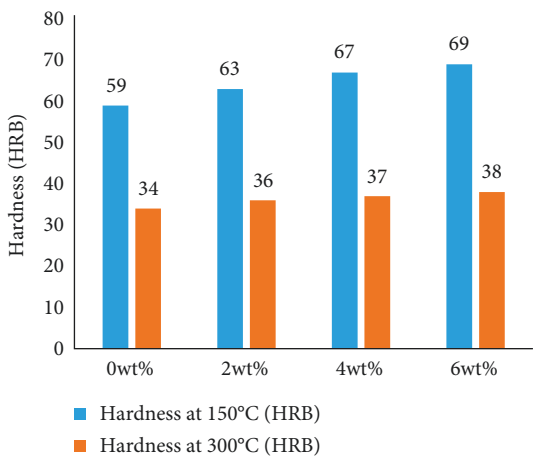

Figure 6: Effect of reinforcing particles on tensile strength of AA7050/Al_2O_3 composites.

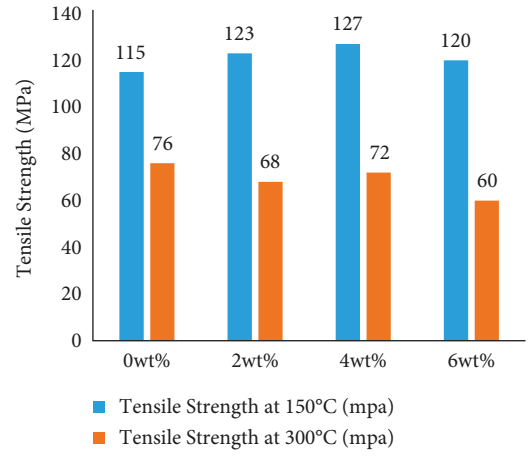

Figure 7: Effect of reinforcing particles on hardness of AA7050/Al_2O_3 composites.

Table 4: ANOVA for altered process parameter.

Level	Reinforcement percentage	Speed (m/s)	Load (N)	Temperature (°C)
1	191.5	191.5	190.8	151.1
2	191.0	191.0	192.8	232.2
3	183.7			
4	198.4			
Delta	14.6	0.5	1.6	82.1
Rank	2	4	3	1

When compared to other composite materials, the AA7050/4Al2O3 composites have a net flow value of 0.386 and have improved material properties at 150°C. The composite AA7050/2Al2O3 performed best at 300°C, with a net flow value of −0.287 [35, 36]. At increased temperatures, the composites show improved mechanical and tribological properties in all cases. The mathematical model for wear was constructed by connecting the results, as indicated in equation (2).

4. Conclusion

The liquid stir casting method was used to successfully create AA7050/Al2O3 composites. Tribological and metallurgical testing on composites was conducted, and the ensuing observations were obtained.

(1) Leading to the generation of a MML, the wear resistance of composites was 7% superior than pure aluminium alloy. When the temperature rises quickly from 150°C to 300°C, the wear rate increases from trivial to severe. At high temperatures, COF decreases as temperature rises, whereas velocity and load have little effect on wear rate.

(2) The insertion of reinforcing particles increases the tensile strength due to Orowan strengthening. When

the temperature is increased to 300°C, the viscosity is reduced by 95%, resulting in a 95% fall in tensile strength.

(3) Because of the Hall–Petch effect, the presence of hard ceramic particles (Al2O3) increases hardness. The ANOVA table revealed that temperature has the utmost impact on material properties, trailed by percent reinforcement. It was important for solar header pipes to use the composite because it has excellent strength at high temperatures.

5. Scope for Future Studies

In the future, tests may be conducted by varying the geometry of the particles and manufacturing them using diverse processes such as Compo casting and squeeze casting.

Data Availability

The data used to support the findings of this study are included within the article.

Conflicts of Interest

The authors declare that they have no conflicts of interest.

References

[1] T. K. Ghosh and M. A. Prelas, "Bioenergy," in *Energy Resources and Systems*, pp. 327–418, Springer, Dordrecht, Netherlands, Europe, 2011.

[2] A. Ummadisingu and M. Soni, "Concentrating solar power - technology, potential and policy in India," *Renewable and Sustainable Energy Reviews*, vol. 15, no. 9, pp. 5169–5175, 2011.

[3] A. Kaminski, B. Vandelle, A. Fave et al., "Aluminium BSF in silicon solar cells," *Solar Energy Materials and Solar Cells*, vol. 72, no. 1-4, pp. 373–379, 2002.

[4] M. Brogren, B. Karlsson, A. Roos, and A. Werner, "Analysis of the effects of outdoor and accelerated ageing on the optical properties of reflector materials for solar energy applications," *Solar Energy Materials and Solar Cells*, vol. 82, no. 4, pp. 491–515, 2004.

[5] R. Bravo, C. Ortiz, R. Chacartegui, and D. Friedrich, "Hybrid solar power plant with thermochemical energy storage: a multi-objective operational optimisation," *Energy Conversion and Management*, vol. 205, Article ID 112421, 2020.

[6] J. Soares and A. C. Oliveira, "Numerical simulation of a hybrid concentrated solar power/biomass mini power plant," *Applied Thermal Engineering*, vol. 111, pp. 1378–1386, 2017.

[7] C. Fenghong, C. Chang, W. Zhenyu, T. Muthuramalingam, and G. Anbuchezhiyan, "Effects of silicon carbide and tungsten carbide in aluminium metal matrix composites," *Silicon*, vol. 11, no. 6, pp. 2625–2632, 2019.

[8] L. Tesfaye, B. Bekele, A. Saka, N. Nagaprasad, K. Sivaramasundaram, and R. Krishnaraj, "Investigating spectroscopic and structural properties of Cr doped TiO2 NPs synthesized through sol gel deposition technique," *Tierarztliche Praxis*, vol. 41, pp. 860–872, 2021.

[9] N. K. Bhoi, H. Singh, and S. Pratap, "Developments in the aluminum metal matrix composites reinforced by micro/nano particles - a review," *Journal of Composite Materials*, vol. 54, no. 6, pp. 813–833, 2020.

[10] P. K. Krishnan, J. V. Christy, R. Arunachalam et al., "Production of aluminum alloy-based metal matrix composites using scrap aluminum alloy and waste materials: influence on microstructure and mechanical properties," *Journal of Alloys and Compounds*, vol. 784, pp. 1047–1061, 2019.

[11] V. Chak, H. Chattopadhyay, and T. L. Dora, "A review on fabrication methods, reinforcements and mechanical properties of aluminum matrix composites," *Journal of Manufacturing Processes*, vol. 56, pp. 1059–1074, 2020.

[12] M. Hoseini and M. Meratian, "Tensile properties of in-situ aluminium-alumina composites," *Materials Letters*, vol. 59, no. 27, pp. 3414–3418, 2005.

[13] J. Hashim, L. Looney, and M. S. J. Hashmi, "Metal matrix composites: production by the stir casting method," *Journal of Materials Processing Technology*, vol. 92-93, pp. 1–7, 1999.

[14] R. Ranjith, P. K. Giridharan, J. Devaraj, and V. Bharath, "Influence of titanium-coated (B4Cp + SiCp) particles on sulphide stress corrosion and wear behaviour of AA7050 hybrid composites (for MLG link)," *Journal of the Australian Ceramic Society*, vol. 53, no. 2, pp. 1017–1025, 2017.

[15] A. Kumar, R. S. Rana, and R. Purohit, "Effect of stirrer design on microstructure of MWCNT and Al alloy by stir casting process," *Advances in Materials and Processing Technologies*, vol. 6, no. 2, pp. 320–327, 2020.

[16] A. Kareem, J. A. Qudeiri, A. Abdudeen, T. Ahammed, and A. Ziout, "A review on AA 6061 metal matrix composites produced by stir casting," *Materials*, vol. 14, no. 1, p. 175, 2021.

[17] S. Sardar, S. Kumar Karmakar, and D. Das, "Tribological properties of Al 7075 alloy and 7075/Al2O3 composite under two-body abrasion: a statistical approach," *Journal of Tribology*, vol. 140, no. 5, Article ID 051602, 2018.

[18] R. Ranjith, P. K. Giridharan, C. Velmurugan, and C. Chinnusamy, "Formation of lubricated tribo layer, grain boundary precipitates, and white spots on titanium-coated graphite-reinforced hybrid composites," *Journal of the Australian Ceramic Society*, vol. 55, no. 3, pp. 645–655, 2019.

[19] S. Sardar, S. K. Karmakar, and D. Das, "Microstructure and tribological performance of alumina–aluminum matrix composites manufactured by enhanced stir casting method," *Journal of Tribology*, vol. 141, no. 4, 2019.

[20] A. Abdollahi, A. Alizadeh, and H. R. Baharvandi, "Comparative studies on the microstructure and mechanical properties of bimodal and trimodal Al2024 based composites," *Materials Science and Engineering A*, vol. 608, pp. 139–148, 2014.

[21] S. Sardar, S. K. Karmakar, and D. Das, "Evaluation of abrasive wear resistance of Al2O3/7075 composite by Taguchi experimental design technique," *Transactions of the Indian Institute of Metals*, vol. 71, no. 8, pp. 1847–1858, 2018.

[22] S. J. S. Chelladurai, R. Arthanari, N. Nithyanandam, K. Rajendran, and K. K. Radhakrishnan, "Investigation of mechanical properties and dry sliding wear behaviour of squeeze cast LM6 aluminium alloy reinforced with copper coated short steel fibers," *Transactions of the Indian Institute of Metals*, vol. 71, no. 4, pp. 813–822, 2018.

[23] S. Sardar, S. K. Pradhan, S. K. Karmakar, and D. Das, "Modeling of abraded surface roughness and wear resistance of aluminum matrix composites," *Journal of Tribology*, vol. 141, no. 7, 2019.

[24] H. Vasudev, L. Thakur, H. Singh, and A. Bansal, "Erosion behaviour of HVOF sprayed Alloy718-nano Al2O3 composite coatings on grey cast iron at elevated temperature conditions,"

Surface Topography: Metrology and Properties, vol. 9, no. 3, Article ID 035022, 2021.

[25] L. Tesfaye Jule, K. Ramaswamy, B. Bekele, A. Saka, and N. Nagaprasad, "Experimental investigation on the impacts of annealing temperatures on titanium dioxide nanoparticles structure, size and optical properties synthesized through sol-gel methods," *Materials Today Proceedings*, vol. 45, pp. 5752–5758, 2021.

[26] M. Vyshakh, R. Krishnaraj, A. P. Sayooj, and M. Afzal, "Experimental investigation on aluminium gravity die casting," *International Journal of Applied Environmental Sciences*, vol. 9, no. 2, pp. 213–222, 2014.

[27] R. Ranjith and P. K. Giridharan, "Experimental investigation of surface hardness and dry sliding wear behavior of AA7050/B4Cp," *High Temperature Material Processes An International Quarterly of High-Technology Plasma Processes*, vol. 19, no. 3-4, pp. 291–305, 2015.

[28] B. Bulcha, J. Leta Tesfaye, D. Anatol et al., "Synthesis of zinc oxide nanoparticles by hydrothermal methods and spectroscopic investigation of ultraviolet radiation protective properties," *Journal of Nanomaterials*, vol. 2021, Article ID 8617290, 10 pages, 2021.

[29] V. Sivamaran, V. Balasubramanian, M. Gopalakrishnan, V. Viswabaskaran, and A. G. Rao, "Identification of appropriate catalyst system for the growth of multi-walled carbon nanotubes via catalytic chemical vapor deposition process in a single step batch technique," *Materials Research Express*, vol. 6, no. 10, Article ID 105620, 2019.

[30] R. Ranjith, P. K. Giridharan, J. Devaraj, and S. Balamurugan, "Frictional behavior of the AA7050/B4cp aluminum composites," *Composites: Mechanics, Computations, Applications, An International Journal*, vol. 9, no. 1, pp. 17–25, 2018.

[31] V. Sivamaran, V. Balasubramanian, M. Gopalakrishnan, V. Viswabaskaran, and A. G. Rao, "Combined synthesis of carbon nanospheres and carbon nanotubes using thermal chemical vapor deposition process," *Chemical Physics Impact*, vol. 4, Article ID 100072, 2022.

[32] S. Venkatesan, B. Visvalingam, G. Mannathusamy, V. Viswanathan, and A. G. Rao, "Effect of chemical vapor deposition parameters on the diameter of multi-walled carbon nanotubes," *International Nano Letters*, vol. 8, no. 4, pp. 297–308, 2018.

[33] S. Venkatesan, B. Visvalingam, G. Mannathusamy, V. Viswanathan, and A. G. Rao, "In situ synthesis of multi-walled carbon nanorings by catalytic chemical vapor deposition process," *International Nano Letters*, vol. 9, no. 2, pp. 119–126, 2019.

[34] V. Sivamaran, D. V. Balasubramanian, D. M. Gopalakrishnan, D. V. Viswabaskaran, D. A. G. Rao, and D. G. Sivakumar, "Mechanical and tribological properties of Self-Lubricating Al 6061 hybrid nano metal matrix composites reinforced by nSiC and MWCNTs," *Surfaces and Interfaces*, vol. 21, Article ID 100781, 2020.

[35] V. Sivamaran, V. Kavimani, M. Bakkiyaraj, and S. T. Selvamani, "Multi response optimization on tribo-mechanical properties of CNTs/nSiC reinforced hybrid Al MMC through RSM approach," *Forces in Mechanics*, vol. 6, Article ID 100069, 2022.

[36] V. Sivamaran, V. Balasubramanian, M. Gopalakrishnan, V. Viswabaskaran, and A. Gouravrao, "Optimizing chemical vapor deposition parameters to attain minimum diameter carbon nano tubes by response surface methodology," *Journal of Advanced Microscopy Research*, vol. 13, no. 2, pp. 181–189, 2018.